



Mapping capability of linear correlation statistics for characterization of complex materials using laser-induced breakdown spectroscopy

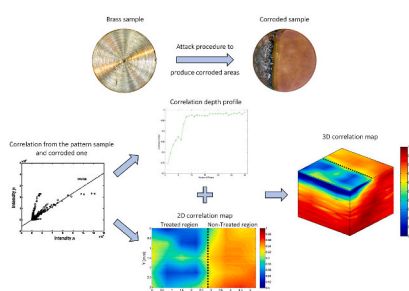
M.P. Mateo, G. Nicolas*

Universidade da Coruña, Campus Industrial, Dpto. Ingeniería Naval e Industrial, Laser Applications Laboratory, C/ Mendizabal s/n, 15403, Ferrol, Spain

HIGHLIGHTS

- Linear correlation statistics applied to LIBS mapping of samples with non-uniform composition on surface and in depth.
- Higher sensitivity to compositional changes by correlation 3D mapping method in comparison with conventional LIBS mapping.
- Location of corroded regions in the analyzed volume of brass samples by correlation 3D mapping analysis.

GRAPHICAL ABSTRACT



ARTICLE INFO

Keywords:

Laser induced breakdown spectroscopy
Depth profiling
3D mapping
Linear correlation coefficient
Corrosion
Brass

ABSTRACT

In this work, the capability of linear correlation statistics for chemical mapping by laser-induced breakdown spectroscopy (LIBS) has been studied for the first time for the characterization of samples with compositional changes on surface and in depth. For that purpose, a corrosion layer of varied spread has been caused in brass samples by chemical treatment and afterwards analyzed by LIBS. Correlation depth profiles, two-dimensional (2D) correlation maps and three-dimensional (3D) correlation maps have been generated from LIBS data to contrast the results obtained from treated and non-treated samples and zones. Conventional LIBS maps based on signal intensity have also been generated for comparison. The conclusions of this study demonstrate the capability and benefits of using the linear correlation method for 3D mapping by LIBS of samples with non-uniform composition. In this sense, the proposed methodology has allowed to determine the location of the corroded regions in the analyzed volume, even in the non-treated zones also affected by the byproducts originated from the chemical attack, in contrast to conventional LIBS mapping based on signal representation.

1. Introduction

Laser-Induced Breakdown Spectroscopy (LIBS) technique provides the characterization of chemical composition based on the analysis of the emission from a laser-induced plasma [1,2]. Among the capabilities of LIBS technique, one of its main features is that the spectral data

extracted from each analysis location can be associated to spatial coordinates [3–5]. This ability allows to obtain information about the elemental composition of the sample associated to a specific path along the sample surface (lateral distribution), along the cross section (depth-profiling) or associated to a certain area of the sample surface (2D chemical map). That characteristic of LIBS technique can be

* Corresponding author.

E-mail address: gines.nicolas@udc.es (G. Nicolas).

<https://doi.org/10.1016/j.aca.2022.340260>

Received 16 May 2022; Received in revised form 22 July 2022; Accepted 11 August 2022

Available online 26 August 2022

0003-2670/© 2022 The Authors. Published by Elsevier B.V. This is an open access article under the CC BY-NC-ND license (<http://creativecommons.org/licenses/by-nc-nd/4.0/>).

exploited to study new and complex materials to understand the relationships between the spatial distribution of chemical elements and the material's properties. In addition, because removal of material is implicit in LIBS experiments, additional equipment is not required for depth-profiling analysis or generation of tomographic maps, that is, at different depth levels. A variety of applications exploiting these spatial capabilities of LIBS to carry out lateral distributions [6–9] and depth-profiling [10,11] can be found in literature. Regarding 2D chemical mapping, LIBS technique is a powerful analytical tool of conductive and nonconductive materials that does not require sample preparation or performing measurements in a vacuum atmosphere [3]. Moreover, lateral and in-depth analysis can be combined in 3D LIBS mapping to provide compositional information corresponding to a certain volume of the sample, although not many contributions have been reported in this mode of analysis [3,12,13], compared to surface mapping and depth-profiling separately.

On the other hand, a review of the bibliography reveals that the results obtained when LIBS data are analyzed by means of statistical tools, such as linear correlation or artificial neural networks, are more robust against experimental fluctuations than those based only on the intensity of a reference line [14,15]. In this sense, correlation statistics have been successfully applied to the comparison of LIB spectra for quantification and classification tasks [14,16–22]. In addition, some studies have already proved that the comparison of LIBS spectra through the linear correlation coefficient provides an improvement of the depth profile quality and the interface localization by minimizing the influence of fluctuations and decay of signals in the global intensity of spectra, caused by sources other than concentration variations [10].

Based on the successful application of correlation statistics to the comparison of LIB spectra for depth profiling and for quantification and classification tasks, the goal of this research has been to study, for the first time to authors' knowledge, the capability and possible benefits of linear correlation applied to LIBS mapping for the characterization of samples where the composition varies on surface and in depth. In order to compare the results obtained through the application of this statistical tool with conventional LIBS mapping based on intensity data, we have continued the study of corrosion and dealloying carried out in a previous work [23]. In that study, several brass specimens, previously subjected to a chemical attack, were analyzed by LIBS and the intensity of Zn I 481.05 nm was plotted in different ways: depth profiles, 2D and 3D maps for the characterization of the corroded areas on the surface and with depth. In the present work, the proposed correlation method has been applied to the same brass samples to determine the location of the corroded regions by generating 3D correlation LIBS maps. In addition, correlation depth profiles and 2D correlation maps have also been plotted for a better explanation of the results through the comparison of treated and non-treated samples. It should be noted that the proposed mapping methodology is not limited to the application chosen as a proof of concept, but it can be extended to other fields of Material Science where pieces with non-uniform composition on surface and in depth require to be characterised with the best degree of precision by LIBS or by other spectroscopic techniques.

2. Materials and methods

2.1. Experimental setup

The experimental setup consisted of a Q-switched Nd:YAG laser (Brilliant, Quantel, pulse width = 5 ns) emitting at 532 nm and a plano-convex quartz lens ($f = 100$ mm) to focus the laser beam at normal incidence onto the sample surface to produce sample ablation and plasma generation. In addition, a fiber optic cable was used to collect the radiation emitted from the plasma into the entrance of an Echelle spectrograph (Mechelle, Andor, spectral coverage from 200 to 850 nm) coupled to an ICCD camera (iStar, Andor). The synchronization of the spectral detection with respect to laser pulse was controlled by a delay

generator (Stanford Research Systems, model DG-535). The experiments were carried out in air, at atmospheric pressure and at a laser pulse energy of 55 mJ that resulted in craters with a diameter of 640 μm . XYZ motorized stages were employed to control the sample movement and the location of the LIBS analysis.

2.2. Sample preparation

To perform this experiment brass was chosen as target material because its behavior under laser pulsed irradiation is quite representative of many materials, and in particular of metals, and because the spectral lines of copper and zinc have been widely studied by LIBS. In addition, oxides found in this material are quite common, which can open up some interesting perspectives for the industrial sector.

Six brass samples (12 mm-diameter, 5 mm-thickness) like the one shown in Fig. 1a, were employed in the experiment. Two of them were not chemically treated: one was used as a pattern or reference sample while the other one was used for comparative purposes and will be denominated control sample hereafter.

In order to obtain different grades of corrosion for the study, specific areas (about half part) of four of the brass samples were treated with a mixture of acetic acid and hydrogen peroxide during increasing exposure times (1, 2, 3 and 6 h corresponding to sample 1 to 4, respectively). As a result of this treatment, a process of oxidation and dezincification has occurred in different grades in the treated brass samples, as shown in Fig. 1b, 1c, 1d and 1e. The attack procedure and the dezincification process have been described in detail in a previous work [23]. It should be noted that the zone of the samples subjected to the chemical treatment corresponds to the left side of the samples in Fig. 1b, 1c, 1d and 1e, and it will be denominated treated region. However, as shown in Fig. 1, the corrosion process has not limited to the treated area of the samples, but it has spread over the entire surface of the sample due to the generation of a foam and other subproducts, formed from the corroded material during the chemical attack of the samples, which affects to the non-immersed area of the samples.

2.3. Experimental methods

2.3.1. Linear correlation

In this study, part of the treated regions and the non-treated ones of the brass samples were analyzed by LIBS and the linear correlation coefficient values were calculated and plotted to detect the corroded zones along the surface and with depth in each sample. For this purpose, the statistical parameter of linear correlation coefficient was checked to avoid the disadvantages observed in some occasions when using intensity values in the conventional mapping approach, like wrong data interpretation due to fluctuations or decay of the plasma signal [10].

Linear correlation measures the degree of interrelation between two variables, x and y , through the linear correlation coefficient, r , calculated using the following formula:

$$r = \frac{\sum_i (x_i - \bar{x})(y_i - \bar{y})}{\sqrt{\sum_i (x_i - \bar{x})^2} \sqrt{\sum_i (y_i - \bar{y})^2}}$$

Where x and y are two data sets, \bar{x} is the mean of all x_i , and \bar{y} is the mean of all y_i [21].

The value of r lies inclusively between -1 and $+1$ and has no units. The absolute value of r can be used as an indication of the association (correlation) between the x and y data sets [14], since the values around zero indicate linearly uncorrelated data sets while $r = 1$ and $r = -1$ correspond to complete positive and negative linear correlation, respectively, which means that the data points lie on a perfect straight line with positive ($r = 1$) and negative ($r = -1$) slopes.

2.3.2. Mapping methodology

LIBS mapping has been carried out under the same irradiation

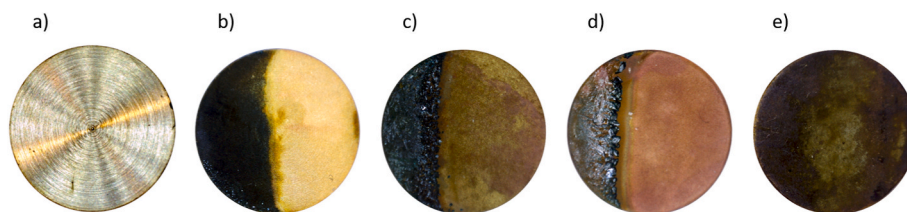


Fig. 1. Optical microscope images of the samples employed in the experiment: (a) Pattern or reference sample. (b) Sample 1. (c) Sample 2. (d) Sample 3. (e) Sample 4.

conditions in samples 1 to 4 and in the pattern sample. For that purpose, 40 positions separated 0.75 mm have been analyzed in each sample, covering a mapped area of 5.25 mm \times 3 mm that includes part of the treated and of the non-treated zones. 30 consecutive in-depth laser pulses have been delivered in each position. Afterwards, correlation coefficient values have been calculated by comparing each spectrum acquired from the analyzed samples with a reference one coming from the pattern sample not subjected to chemical attack, that is, free of corrosion.

3. Results and discussion

Based on the successful application of correlation statistics to the comparison of LIB spectra for quantification and classification tasks, the goal of this research was to study the possibility of using a simple linear correlation approach for distinguishing variations of composition over the entire volume of a sample through the generation of correlation LIBS maps. For this purpose, the linear correlation coefficient was employed for the comparison of spectra obtained from the LIBS analysis of the brass specimens. For the calculus of correlation coefficient values, the spectral intensities (y_i) corresponding to a LIB spectrum y were plotted against intensities (x_i) of a LIB spectrum x . In this way, each point in the generated plots corresponds to a pair of intensity values (x_i , y_i) at the same wavelength i . Some examples of the resulting correlation plots are shown in Fig. 2. On the one hand, Fig. 2a shows a typical correlation graph corresponding to a couple of very similar spectra. On the other hand, Fig. 2b shows a correlation graph of two spectra that are quite different. In the case of Fig. 2a, both spectra were acquired from non-treated samples (reference and control samples) and data points can be fitted to a straight line. However, one of the spectra of Fig. 2b was acquired from a non-treated sample (pattern sample) whereas the other one was acquired from the corroded area of a treated sample. Consequently, the absolute value of the correlation coefficient, r , calculated using the equation included in section 2.3.1, is around 1 (0.9898) in the case of Fig. 2a and lower (0.7209) in the case of Fig. 2b.

In order to contrast the results obtained through the application of this statistical tool with other ones based only in the intensity data, we have continued the study of corrosion and dealloying carried out in a previous paper [23] in six brass samples treated with acetic acid and hydrogen peroxide. This treatment caused a process of corrosion called dezincification or selective-leaching over a region of the samples (Fig. 1).

With the aim of studying the extent of the corrosion process by LIBS in the surface and with depth, a mapping process has been carried out in samples 1 to 4 and, for comparison, in the pattern sample, following the mapping methodology explained in section 2.3.2. In order to test the mapping capability of the proposed correlation method by characterizing the spread of corrosion process, we have used three different plotting methods based on the application of correlation statistics to the analysis of LIBS spectra: depth profiles, 2D maps and 3D maps.

3.1. Correlation depth profiles

In LIBS depth profiling, successive laser shots (30 in this study) are delivered on the same position of the sample to analyze the variation of the composition with depth. In this way, each acquired spectrum corresponds to a certain eroded layer of material or depth. For the calculus of the correlation coefficient, a reference spectrum taken from the analysis of the surface of the pattern sample was chosen in this study as the representative spectrum of a layer free of corrosion. Finally, the absolute value of the linear correlation coefficient was calculated by comparison of both, the reference spectrum and each one of the 30 spectra of the sample in-depth analysis sequence. It should be noted that the same reference spectrum from the surface of the pattern sample was used for that comparison, instead of using a different one for each depth level. The reason is that r is known to be insensitive to the linear transformation of any or both of the two data sets for which it is calculated [14]. Therefore, r value is not influenced by those circumstances that affect the spectra uniformly, like experimental factors and sources other than concentration variations which can cause

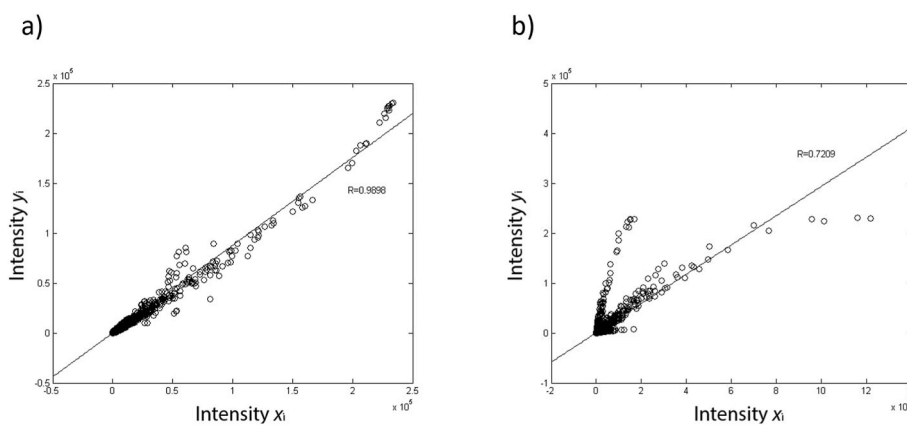


Fig. 2. (a) Correlation graph of two spectra acquired from non-treated samples (pattern and control samples) showing the fitting of data to a straight line. (b) Correlation graph of two spectra acquired one from the pattern sample and another one from the corroded area of a treated sample as an example of low value of the correlation coefficient.

fluctuations or decay of the global spectral intensity. In this sense, as it was demonstrated in a previous work [10], the comparison of LIBS spectra through the linear correlation coefficient avoids some problems of the classical depth profiling approach based on intensity evolution, such as scattered points and decrease in the intensity profile owing to pulse-to-pulse fluctuations and loss of emission signal with depth, respectively. These advantages of correlation calculus make unnecessary to use a different reference spectrum at each depth level for the calculus of r because, as the composition of the reference sample is homogeneous with depth, if there is a change in the spectral intensity of the reference sample due to depth, it will affect the whole spectrum but not significantly to r calculus. Therefore, the resulting r values should be practically the same whatever reference spectrum chosen for the comparison with the spectra from the treated samples.

In order to generate the correlation depth profiles for the corrosion study, the r values obtained by comparing the reference spectrum and each one of the 30 spectra of the in-depth sequence of the treated samples were plotted in a graph. The result was a depth profile in which the value of the linear correlation coefficient was plotted in the Y-axis and the number of laser pulses was plotted in the X-axis. As an example, Fig. 3 shows two correlation depth profiles corresponding to one in-depth analysis carried out in the treated area in sample 3 (Fig. 3a) and in the control sample (Fig. 3b), as examples of correlation depth profiles corresponding to a corroded sample and to a sample free of corrosion, respectively. As it can be seen, there is a clear difference between both correlation depth profiles. On the one hand, in the case of the correlation depth profile of the treated sample, shown in Fig. 3a, the absolute value of the correlation coefficient increases during the first eight pulses because of the progressive removal of the corrosion layer. Then, its value remains almost constant around 1 because the spectra corresponding to the 9th to 30th pulses are almost identical to the reference spectrum obtained from the pattern sample. In this way, it is possible to estimate the reach of the corrosion layer. However, in the case of the correlation depth profile from the control sample displayed in Fig. 3b, the value of the correlation coefficient is approximately 1 along all the ablation process due to the similarity of the spectra of the depth sequence with the reference spectrum. As shown, the correlation depth profiles allow to distinguish accurately between corroded layers and those which are free of corrosion. In addition, if the ablation rate is calculated, it is possible to express the X axis in the profiles in micrometers instead of number of pulses and therefore to estimate the thickness of the corroded layer from the correlation profiles. In this sense, average ablation rates were calculated for each sample like in our previous work [23], resulting in an estimation of corrosion thickness around 85 μm , with small differences of less than ten microns above and below, depending on the sample.

3.2. 2D correlation maps

The correlation depth profile has been proved as a good method to study the depth extent of the corrosion layer in a single point of the sample. Nevertheless, the corrosion area is not present along all the surface of the sample. At this regard, 2D correlation maps have been generated in this study to obtain information about compositional variations in the surface of the sample, in this case, the exact location of the corroded regions. In 2D LIBS maps, successive individual analyses are performed in adjacent positions at the same depth level of the sample, usually the surface, and they are associated to spatial coordinates. In this study, spectral data extracted from each analysis location have been compared with the reference spectrum from the pattern sample to obtain the values of the correlation coefficient along the surface of the samples. Finally, these values have been plotted in form of 2D correlation maps where the color indicates the value of the correlation coefficient while the spatial information is in the X-Y axis. As an example, a correlation map of the surface of sample 2 is shown in Fig. 4a, corresponding to a mapped area of 5.25 mm \times 3 mm. As it can be observed in that map, the chemically-treated region (left zone), exhibits lower values of the correlation coefficient, below 0.9 in most cases, and close to 0.8 in some zones, than the non-treated one (right zone). These lower values are due to the significant differences between the reference spectrum, obtained from the surface of the pattern sample, and the spectra from the attacked zone of sample 2, because of the compositional modifications due to the corrosion process. In contrast, the spectra from the non-treated region of sample 2 are more similar to the reference spectrum and therefore the correlation values are higher, around 0.94 (yellow-orange color). However, it should be pointed out that the correlation coefficients corresponding to the area of sample 2 that was not submerged in the chemical bath are lower than expected, as evidenced from comparison with the correlation map of the surface of the reference sample plotted in Fig. 4b, with values around 1 (red color). That is because, despite not being submerged in the chemical bath and therefore not directly attacked, the right region of sample 2 was slightly affected by the byproducts originated from the treatment (foam, vapor ...) leading, as a consequence, to small differences of the corresponding spectra with the reference one. This explanation is supported by the appearance of the surface of sample 2 compared to the reference sample, as shown in Fig. 1, where the right side of samples 1–4 has also been modified by the chemical treatment.

Once demonstrated the capability of 2D correlation maps for the characterization of compositional variations in the surface of the sample, the next step is to compare the proposed correlation mapping procedure with the conventional one based on signal intensity. For that purpose, the intensity of the emission line of Zn I 481.05 nm has been plotted in Fig. 4 in form of 2D intensity maps: Fig. 4c and d,

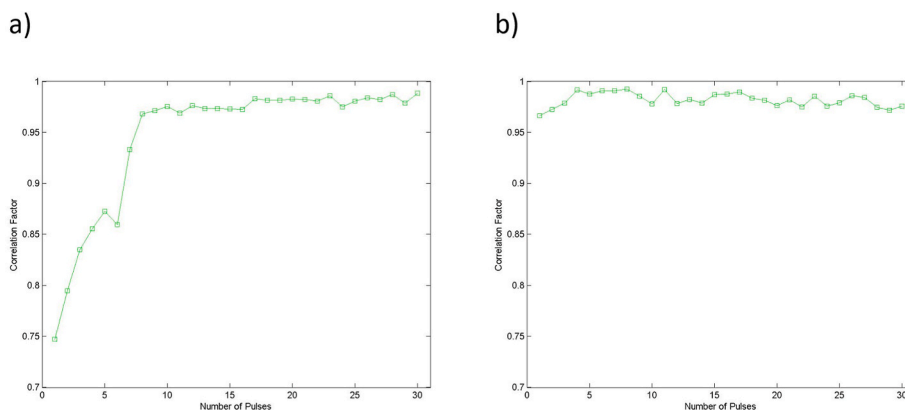


Fig. 3. Depth analysis of brass samples corresponding to 30 in-depth laser pulses. (a) Correlation depth profile of the treated zone of sample 3 (corroded sample). (b) Correlation depth profile of the control sample (non-corroded sample).

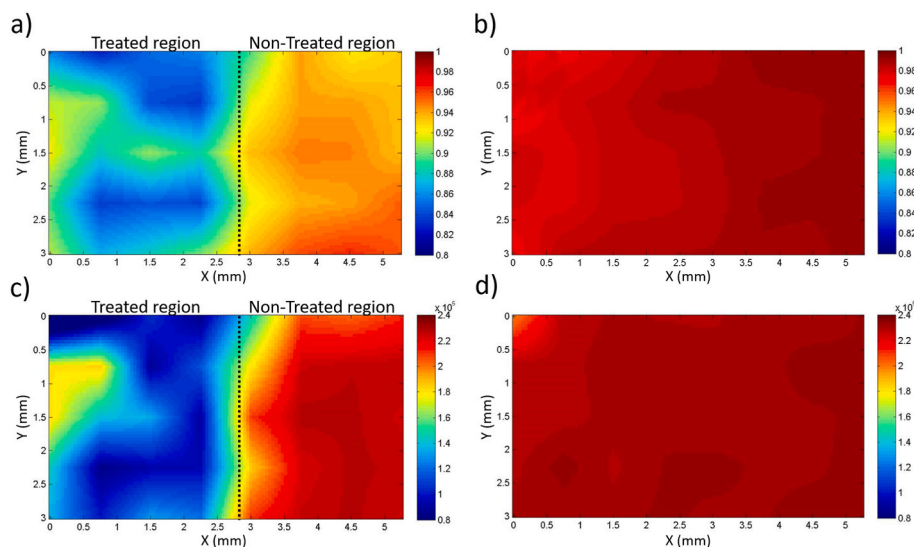


Fig. 4. (a) 2D correlation map corresponding to the surface of sample 2. (b) 2D correlation map corresponding to the surface of pattern sample (c) 2D intensity map of Zn I 481.05 nm corresponding to the surface of sample 2. (d) 2D intensity map of Zn I 481.05 nm corresponding to the surface of pattern sample. Color bar indicates values of the linear correlation coefficient in (a) and (b) and values of intensity in (c) and (d). The approximate location of the boundary between the treated and the non-treated regions of sample 2 has been indicated by a dotted line, for clarification. (For interpretation of the references to color in this figure legend, the reader is referred to the Web version of this article.)

corresponding to the map from the surface of sample 2 and from that of the reference sample, respectively. It should be clarified that maps of Fig. 4 are the result of different ways of processing or plotting (correlation or intensity maps) the data obtained from the analysis of sample 2 (Fig. 4a and c), and of the reference sample (Fig. 4b and d). As shown in Fig. 4c, the treated region of the sample (left side) exhibits a lower intensity of Zn than the non-treated one due to the dezincification of the brass caused by the chemical attack of the sample [23]. On the other hand, the intensity values of the right side of the map, corresponding to the non-treated region, are very similar to those of the intensity map of Fig. 4d obtained from the reference sample, that is, the sample that has not been subjected to the corrosion treatment. In this sense, in the intensity map of Fig. 4c there is no evidence of corrosion process in the non-treated region, in contrast to the correlation map of Fig. 4a, demonstrating the higher sensitivity of the mapping procedure based on correlation as compared to conventional one or standard maps based on intensity.

3.3. 3D correlation maps

When the composition of the sample is not uniform on the surface nor with depth, like in the case of the corrosion layer of the samples used in this study, it cannot be totally characterized by LIBS through a 2D map or a depth profile. For that reason, LIBS depth profiles and 2D maps were combined in this work by a home-made software based on the application of correlation statistics to the analysis of LIBS spectra to plot the linear correlation coefficients in the format of 3D maps. In this way, the 3D correlation maps generated provided information about compositional changes corresponding to the analyzed volume of the samples, allowing the estimation of the reach and location of the corrosion layer.

Fig. 5 displays the 3D correlation maps generated from all the treated samples, where the vertical axes correspond to depth, being therefore the surface located at the top of the map and corresponding to a mapped area of 5.25 mm × 3 mm. In those maps, the treated zone is located at

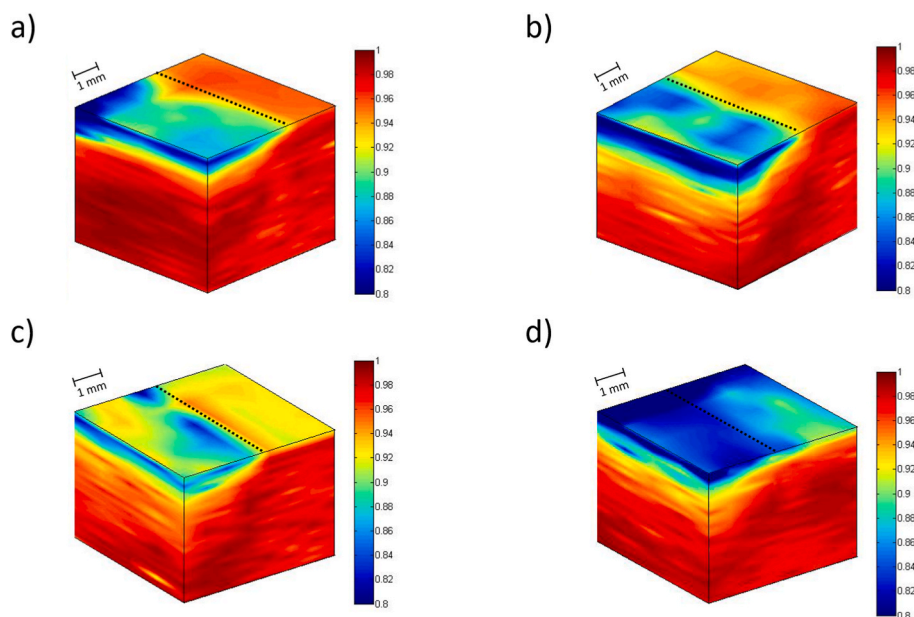


Fig. 5. 3D correlation maps: (a) Sample 1. (b) Sample 2. (c) Sample 3. (d) Sample 4. The approximate location of the boundary between the treated and the non-treated regions of the samples has been indicated by a dotted line, for clarification. Color bars indicate values of the linear correlation coefficient. (For interpretation of the references to color in this figure legend, the reader is referred to the Web version of this article.)

the left side of the dotted line that indicates the approximate location of the boundary between the treated and the non-treated regions. As shown in Fig. 5, the location of the corroded regions in the analyzed volume can be distinguished easily by means of the correlation coefficient plotted as a color scale. Correlation coefficient values between 0.8 and 1 are plotted from blue to red color, depending on the degree of corrosion. In Fig. 5, the red color assigned to correlation coefficients close to 1, corresponds to regions with a LIBS spectrum, and therefore chemical composition, very similar to that of the reference spectrum acquired from the pattern sample, that is, free of corrosion. On the other hand, blue colors are assigned to the lowest correlation values which have been obtained from the highly corroded regions. As shown, the response is quite similar in the four samples, although some differences can be observed as the exposure time to the corrosion attack is increased (from sample 1 to 4), especially in the zones which were not submerged in the chemical bath.

As in the previous section, it should be highlighted that the part of the samples that was not immersed in the chemical mixture was also affected by the corrosion process. This effect is evident in the maps of the four samples of Fig. 5, where the non-submerged zones exhibit colors different to the red that is characteristic of a non-corroded sample. Indeed, the correlation value in the non-treated zone of the samples decreases from sample 1 to 4, indicating a higher degree of corrosion when the exposure time is increased. It can also be observed in Fig. 5 that the corrosion in the non-treated zones affects only to the outer layer of the sample, in contrast to the treated zones where low correlation coefficients have been obtained deeper. On the contrary, in the 3D standard maps of the previous study [23], the effect of chemicals over the non-treated region was only perceptible in the sample with the longest treatment time, sample 4, indicating a lower sensibility to compositional changes of the conventional method compared to the proposed one. These results demonstrate the capability and benefits of 3D correlation mapping for characterizing compositional variations in a volume, like the localization of non-uniform corrosion layers.

4. Conclusions

The capability of linear correlation for LIBS mapping and the advantages of this new kind of maps over standard maps, based only in the LIBS signal intensity, have been studied in this work. For that purpose, brass specimens with a corrosion layer covering to a greater or lesser extent the metal surface have been analyzed.

Firstly, correlation depth profiles have been used to study the extent of the corrosion layer with depth. Moreover, 2D correlation maps have been generated to locate the region of the sample surface affected by the chemical attack. In both types of graphs, the results obtained from treated and non-treated samples have been compared. Finally, with the aim of characterizing the spread of the corrosion process over the sample volume and of testing its analytical capability, 3D correlation maps have been plotted by combining 2D correlation maps and correlation depth profiles. In those 3D maps, the correlation coefficient plotted as a color scale has allowed to determine the location of the corroded regions in the analyzed volume, even in the non-treated zones also affected by the byproducts originated from the chemical attack, in contrast to conventional mapping.

The results of this study have proven the capability of the linear correlation for LIBS mapping of samples with non-uniform composition on surface and in depth. In particular, it has been successfully tested to locate corroded regions at different depths and areas of brass samples. Moreover, the application of this statistical tool provides additional information in comparison with conventional LIBS mapping based on intensity, since it improves the sensitivity and the accuracy of LIBS technique to discriminate regions with slightly different composition.

CRediT authorship contribution statement

M.P. Mateo: Conceptualization, Data curation, Methodology, Writing – original draft, Writing – review & editing. **G. Nicolas:** Conceptualization, Methodology, Supervision, Writing – original draft, Writing – review & editing.

Declaration of competing interest

The authors declare that they have no known competing financial interests or personal relationships that could have appeared to influence the work reported in this paper.

Data availability

Data will be made available on request.

Acknowledgement

The authors want to thank Rafael Cerrato and Alejandro Casal, students of Universidade da Coruña, for their contribution in the data acquisition and processing.

References

- [1] A.W. Miziolek, V. Palleschi, I. Schechter, *Laser-induced Breakdown Spectroscopy (LIBS): Fundamentals and Applications*, first ed., Cambridge University Press, Cambridge, 2006.
- [2] D.A. Cremers, L.J. Radziemski, *Handbook of Laser-Induced Breakdown Spectroscopy, First*, John Wiley & Sons Ltd, Oxford, UK, 2006.
- [3] V. Piñon, M.P. Mateo, G. Nicolas, Laser-induced breakdown spectroscopy for chemical mapping of materials, *Appl. Spectrosc. Rev.* 48 (2013) 357–383, <https://doi.org/10.1080/05704928.2012.717569>.
- [4] D.A. Cremers, R.C. Chinni, Laser-induced breakdown spectroscopy—capabilities and limitations, *Appl. Spectrosc. Rev.* 44 (2009) 457–506, <https://doi.org/10.1080/05704920903058755>.
- [5] L. Jolivet, M. Leprince, S. Moncayo, L. Sorbier, C.-P. Lienemann, V. Motto-Ros, Review of the recent advances and applications of LIBS-based imaging, *Spectrochim. Acta Part B At. Spectrosc.* 151 (2019) 41–53, <https://doi.org/10.1016/j.sab.2018.11.008>.
- [6] F.J. Fortes, I. Vadillo, H. Stoll, M. Jiménez-Sánchez, A. Moreno, J.J. Laserna, Spatial distribution of paleoclimatic proxies in stalagmite slabs using laser-induced breakdown spectroscopy, *J. Anal. At. Spectrom.* 27 (2012) 868, <https://doi.org/10.1039/c2ja10299d>.
- [7] J.A. Varela, J.M. Amado, M.J. Tobar, M.P. Mateo, A. Yañez, G. Nicolas, Characterization of hard coatings produced by laser cladding using laser-induced breakdown spectroscopy technique, *Appl. Surf. Sci.* 336 (2015) 396–400.
- [8] Ş. Yalçın, S. Örer, R. Turan, 2-D analysis of Ge implanted SiO₂ surfaces by laser-induced breakdown spectroscopy, *Spectrochim. Acta Part B At. Spectrosc.* 63 (2008) 1130–1138, <https://doi.org/10.1016/j.sab.2008.09.002>.
- [9] P. Škarková, K. Novotný, P. Lubal, A. Jebavá, P. Pořízka, J. Klus, Z. Farka, A. Hrdlička, J. Kaiser, 2d distribution mapping of quantum dots injected onto filtration paper by laser-induced breakdown spectroscopy, *Spectrochim. Acta Part B At. Spectrosc.* 63 (2008) 1130–1138, <https://doi.org/10.1016/j.sab.2017.03.016>.
- [10] M.P. Mateo, G. Nicolas, V. Piñon, A. Yañez, Improvements in depth-profiling of thick samples by laser-induced breakdown spectroscopy using linear correlation, *Surf. Interface Anal.* 38 (2006) 941–948, <https://doi.org/10.1002/sia>.
- [11] T. Ctvrtnickova, F.J. Fortes, L.M. Cabalin, V. Kanický, J.J. Laserna, Depth profiles of ceramic tiles by using orthogonal double-pulse laser induced breakdown spectrometry, *Surf. Interface Anal.* 41 (2009) 714–719, <https://doi.org/10.1002/sia.3077>.
- [12] I. Lopez-Quintas, M.P. Mateo, V. Piñon, A. Yañez, G. Nicolas, Mapping of mechanical specimens by laser induced breakdown spectroscopy method: application to an engine valve, *Spectrochim. Acta Part B At. Spectrosc.* 74–75 (2012) 109–114, <https://doi.org/10.1016/j.sab.2012.06.035>.
- [13] G. Nicolas, M.P. Mateo, V. Piñon, 3D chemical maps of non-flat surfaces by laser-induced breakdown spectroscopy, *J. Anal. At. Spectrom.* 22 (2007) 1244, <https://doi.org/10.1039/b704682k>.
- [14] G. Galbács, I.B. Gornushkin, B.W. Smith, J.D. Winefordner, Semi-quantitative analysis of binary alloys using laser-induced breakdown spectroscopy and a new calibration approach based on linear correlation, *Spectrochim. Acta Part B At. Spectrosc.* 56 (2001) 1159–1173, [https://doi.org/10.1016/S0584-8547\(01\)00205-1](https://doi.org/10.1016/S0584-8547(01)00205-1).
- [15] S. Pagnotta, E. Grifoni, S. Legnaioli, M. Lezzerini, G. Lorenzetti, V. Palleschi, Comparison of brass alloys composition by laser-induced breakdown spectroscopy and self-organizing maps, *Spectrochim. Acta Part B At. Spectrosc.* 103–104 (2015) 70–75, <https://doi.org/10.1016/j.sab.2014.11.008>.

- [16] A.J. López, G. Nicolás, M.P. Mateo, A. Ramil, V. Piñón, A. Yáñez, LIPS and linear correlation analysis applied to the classification of Roman pottery Terra Sigillata, *Appl. Phys. Mater. Sci. Process* 83 (2006) 695–698, <https://doi.org/10.1007/s00339-006-3556-6>.
- [17] I.B. Gornushkin, A. Ruíz-Medina, J.M. Anzano, B.W. Smith, J.D. Winefordner, Identification of particulate materials by correlation analysis using a microscopic laser induced breakdown spectrometer, *J. Anal. At. Spectrom.* 15 (2000) 581–586, <https://doi.org/10.1039/a909873i>.
- [18] I.B. Gornushkin, B.W. Smith, H. Nasajpour, J.D. Winefordner, Identification of solid materials by correlation analysis using a microscopic laser-induced plasma spectrometer, *Anal. Chem.* 71 (1999) 5157–5164, <https://doi.org/10.1021/ac9905524>.
- [19] R.J. Lasheras, C. Bello-Gálvez, J. Anzano, Identification of polymers by LIBS using methods of correlation and normalized coordinates, *Polym. Test.* 29 (2010) 1057–1064, <https://doi.org/10.1016/j.polymertesting.2010.07.011>.
- [20] G. Galbács, I.B. Gornushkin, J.D. Winefordner, Generalization of a new calibration method based on linear correlation, *Talanta* 63 (2004) 351–357, <https://doi.org/10.1016/j.talanta.2003.11.009>.
- [21] J.M. Anzano, I.B. Gornushkin, B.W. Smith, J.D. Winefordner, Laser-induced plasma spectroscopy for plastic identification, *Polym. Eng. Sci.* 40 (2000) 2423–2429, <https://doi.org/10.1002/pen.11374>.
- [22] A. Ferrero, P. Lucena, R.G. Herrera, A. Doña, R. Fernández-Reyes, J.J. Laserna, Libraries for spectrum identification: method of normalized coordinates versus linear correlation, *Spectrochim. Acta Part B At. Spectrosc.* 63 (2008) 383–388, <https://doi.org/10.1016/j.sab.2007.11.040>.
- [23] R. Cerrato, A. Casal, M.P. Mateo, G. Nicolas, Dealloying evidence on corroded brass by laser-induced breakdown spectroscopy mapping and depth profiling measurements, *Spectrochim. Acta Part B At. Spectrosc.* 130 (2017) 1–6, <https://doi.org/10.1016/j.sab.2016.11.006>.